

NUMERICAL SIMULATION OF FLOWS IN AN ENGINE CYLINDER WITH AN
ECCENTRIC DEEP BOWL COMBUSTION CHAMBER DURING COMPRESSION
(1st Report, FORMULATION AND ALGORITHM)

محاكاة عددية للسريان داخل اسطوانة ذات غرفة احتراق غير مركزية في المكبس

خلال شوط الانضغاط (التقرير الأول : التكوين والنموذج العددي)

By

M.S. El Kady¹, H.J. Mascheck² and A. Hoche³

الخلاصة - هذا البحث يشرح خطوة أخرى في تقديم نموذج عددي وطريقة عددية لاستنباط حركة الغاز في اسطوانة محرك ترددي . في المرجع (١) تم دراسة حركة الغاز في غرفة احتراق مركزية مع محور الاسطوانة . أما في هذا البحث فقد تم انحراف غرفة الاحتراق لتكون غير مركزية ووضعت المعادلات التي تصعب حركة الغاز الغير مستقر ثلاثي الأبعاد خلال شوط الانضغاط . وباستخدام طريقة الرسم المتوافق تم اختيار نظام إحداثيات خاص تكون فيه الفتحة الغير مركزية بها مركزية مع محور الاسطوانة وبمساعدة ذلك وباستخدام طريقة التحويلات تم مفكوك فورير للمتغيرات تحولت المشكلة من ثلاثية الأبعاد الى مجموعة من المشاكل ثنائية الأبعاد المرتبطة معا . وخلال عملية النمذجة العددية استخدمت طريقة الفروق المحدودة واستخدم فيها نظام الشبكة المتحركة وطريقة الاتجاه المتغير صريح وذلك لعملية تصحيح اللفظ بواسطة التكرار . وقد صمم برنامج كومبيوتر لمحاكاة حركة الغاز ثلاثية الأبعاد الغير مستقر داخل اسطوانة ذات غرفة احتراق عميقة غير مركزية خلال شوط الانضغاط . وفي المرجع (١١) تم استخدام هذا البرنامج في مجال عددي على احدى ساكينات الديزل الصغيرة وعرض النتائج ودراساتها .

ABSTRACT

This paper describes another step in the numerical simulation of the in-cylinder gas flow in the real reciprocating engine cylinder. The deep bowl combustion chamber in the piston which is axisymmetric in (1) is shifted here to be eccentric to the cylinder axis and the three dimensional unsteady air motion during the compression stroke is predicted. By the use of the conformal mapping a special coordinate system is chosen in order to make the eccentric bowl axisymmetric, then by the use of the perturbation method and Fourier expansion for the dependent variables the three dimensional problem is transferred to a group of two-dimensional problems which are bounded together. Predictions were carried out using a finite difference method to solve the

1. Mech. Power Dept., Faculty of Engineering, Mansoura University
2. Professor, Institute of Fluid Mechanics, Technical University of Dresden, Germany (GDR)
3. Professor and head of the institute of I.C.E., Technical University of Dresden, Germany (GDR)

governing differential equations for continuity and momentum. A movable grid system is employed and the alternating direction implicit method (ADI) was used for the pressure correction. A computer program system EBSTR was developed for this case. In the second report numerical computation is made for a typical case and the results are discussed briefly [11].

1. INTRODUCTION

The investigation of the gas flows in the cylinder of the internal combustion engine is one of the most important ways to realize low pollution and high combustion efficiency. Since the in-cylinder flows are in a very complicated three dimensional turbulent state, there are many barriers to reveal the flow only by experimental study. Therefore, recently the method of flow analysis by a computer has been developed. So far, however, most of the flow analysis have been performed on the axisymmetric or two dimensional flows [1]-[7].

The aim of this study is to simulate numerically the three-dimensional flow of the eccentric deep bowl combustion chamber of the direct injection diesel engine during the compression stroke. This is another step in approach to the gas flow in the real cylinder of the four stroke engines by making the deep bowl in piston which is axisymmetric in [1] eccentric to the cylinder axis. This part of the paper describes the formulation of the problem and the method of the numerical analysis, while the second part [11] gives the results of sample calculation for a typical small direct injection diesel engine.

2. MATHEMATICAL MODEL

2.1. Coordinate system

A special coordinate system (R, θ, z) is chosen in which the eccentric deep bowl combustion chamber will be axisymmetric, this will make the boundary conditions easy to be handled and also the discretisation error will be very near to zero. The cylinder wall and also the bowl wall will have constant radial values $R_c = \text{const.}$ This will be done by the conformal mapping as shown in Fig. 1-3. The zero point of this coordinate system does not coincide with the center of the bowl or the center of the cylinder as shown in figures 2 and 3 but it lies at the symmetrical plane at $x = -\epsilon$ where ϵ is an eccentric parameter which is assumed to be small. As the eccentric parameter ϵ tends to be zero the bowl axis tends to coincide with the cylinder axis and also with the z -axis of the coordinate system R, θ, z and when $\epsilon = 0$ the coordinate system R, θ, z will coincide with the normal cylindrical system. To do this, we define first in the z plane the complex variables w, ζ as follows

$$w = x + iy \quad \text{and} \quad \zeta = \xi + i\eta$$

where $\zeta = (w + \epsilon) / (\epsilon w + 1)$ and the reciprocal $w = (\zeta - \epsilon) / (1 - \zeta \epsilon)$.
In these planes the circle $|\zeta| = 1$ and $|\zeta|^2 = R_b^2$ in the ζ -plane

represent as shown in figure 2 the circles $|w|=1$ and $|w(\zeta)+a|^2=R_D^2 =$ constant in the w -plane. For these relations the variables ξ, R and θ can be expressed as a function of a, x, r_D and y .

2.2 Governing equations

The fluid density is assumed to be spatially uniform over the flow field but time dependent. The true flow field inside real internal combustion engines might be reasonably modeled via a large inviscid core plus a very small viscous boundary layer at the walls, as conventionally done in aerodynamics. Thus the inviscid flow is investigated here.

The governing equations will be the continuity and Euler equations. For the cartesian coordinate X, Y, Z which will be oriented at every point due to the direction of the coordinates $R = \text{constant}$ and $\theta = \text{constant}$ as shown in Fig. 4 the differential equations will take, like in any cartesian coordinates, the form:

$$\begin{aligned} \frac{\partial U}{\partial t} + U \frac{\partial U}{\partial x} + V \frac{\partial U}{\partial y} + W \frac{\partial U}{\partial z} + \frac{\partial P}{\partial x} &= 0 \\ \frac{\partial V}{\partial t} + U \frac{\partial V}{\partial x} + V \frac{\partial V}{\partial y} + W \frac{\partial V}{\partial z} + \frac{\partial P}{\partial y} &= 0 \end{aligned} \quad (1)$$

$$\begin{aligned} \frac{\partial W}{\partial t} + U \frac{\partial W}{\partial x} + V \frac{\partial W}{\partial y} + W \frac{\partial W}{\partial z} + \frac{\partial P}{\partial z} &= 0 \\ \frac{\partial U}{\partial x} + \frac{\partial V}{\partial y} + \frac{\partial W}{\partial z} + \frac{1}{\rho} \frac{d\rho}{dt} &= 0 \end{aligned} \quad (2)$$

where P is the pressure divided by the density

If θ is the angle between the coordinate axis $R = \text{const.}$ and $X = \text{const.}$ as shown in Fig. 4, the relation between the velocity components u, v, w in the coordinate system R, θ, z and U, V, W in the coordinate system X, Y, Z will take the form:

$$\begin{aligned} U &= u \cos \theta - v \sin \theta \\ V &= u \sin \theta + v \cos \theta \\ W &= w \end{aligned} \quad (3)$$

Using equation (3) and the relations between the two coordinate systems the governing equations (1) and (2) can be transformed and written in the coordinate system R, θ, z as follows:

$$\begin{aligned} \frac{\partial u}{\partial t} + u \frac{\partial u}{\partial R} \gamma - u \cdot v \cdot \frac{\partial \theta}{\partial R} + v \cdot \frac{\gamma}{R} \frac{\partial u}{\partial \theta} - v^2 \cdot \frac{\gamma}{R} \frac{\partial \theta}{\partial \theta} + w \frac{\partial u}{\partial z} + \gamma \frac{\partial P}{\partial R} &= 0 \\ \frac{\partial v}{\partial t} + u \cdot \gamma \left[u \frac{\partial \theta}{\partial R} + \frac{\partial v}{\partial R} \right] + v \cdot \frac{\gamma}{R} \left[\frac{\partial v}{\partial \theta} + u \frac{\partial \theta}{\partial \theta} \right] + w \frac{\partial v}{\partial z} + \frac{\gamma}{R} \frac{\partial P}{\partial \theta} &= 0 \quad (4) \\ \frac{\partial w}{\partial t} + u \cdot \gamma \cdot \frac{\partial w}{\partial R} + v \cdot \frac{\gamma}{R} \frac{\partial w}{\partial \theta} + w \frac{\partial w}{\partial z} + \frac{\partial P}{\partial z} &= 0 \end{aligned}$$

$$\frac{\partial u}{\partial R} + \frac{\gamma}{R} \frac{\partial v}{\partial \theta} + \frac{\partial w}{\partial z} - v \cdot \gamma \cdot \frac{\partial B}{\partial R} + \frac{1}{R} \frac{dQ}{dt} = 0$$

$$\text{where } \gamma = \frac{1 - 2\epsilon R \cos\theta + \epsilon^2 R^2}{1 - \epsilon^2}$$

2.3 Integration area

Figures 1 and 4 show the integration area with its boundaries which consists of the axis, cylinder head, cylinder wall, piston crown, bowl wall and bowl bottom.

During the motion of the piston in a fixed z coordinate the boundaries of the integration area will vary with the time. To avoid an incomplete coverage of the wall boundaries in the computational grid which will be discussed in 3.2. a movable coordinate z' is used in the axial direction to make the boundaries of the integration area time independent where

$$z' = \frac{z}{h} c_1 \quad 0 \leq z' \leq c_1, \quad 0 \leq z \leq h$$

$$z' = z + c_1 - h \quad c_1 \leq z' \leq c_1 + b_1, \quad h \leq z \leq h + b_1$$

The governing equations will be transformed to the time movable coordinate system in which every point has an axial velocity in the cylinder, that is the same velocity of the grid point w_g in Fig.4. The time derivative for the movable coordinate will take the following form:

$$\left. \frac{\partial}{\partial t} \right|_{\text{mov}} = \left. \frac{\partial}{\partial t} \right|_{\text{fixed}} + w_g \frac{\partial}{\partial z} \quad (5)$$

$$\text{where } w_g = \frac{z}{h} w_p \quad \text{for } 0 \leq z \leq h$$

$$\text{and } w_g = w_p \quad \text{for } h \leq z \leq h + b_1$$

This will change the governing equation (4) by only an excess derivative term in the convection form in the axial direction.

2.4 Governing equations by small eccentricity of the bowl

Equations (4) will be solved by the perturbation method. Taking the eccentricity as a small perturbation parameter and restricting the solution on the linear terms of ϵ , the velocity components u, v, w and the pressure P can be written in the following form:

$$F(R, \theta, z) = F_0(R, z) + \epsilon F_1(R, \theta, z) \quad (6)$$

The first term $F_0(R, \theta)$ represents the independent term of θ for the velocities u, v, w and the pressure P . This term casts

the symmetrical flow (the main flow). The second term $F_1(R, \theta, z)$ represents the additional term which expresses the deviation of the flow from the symmetrical case (the disturbance term).

The additional terms for the velocities and the pressure which depend on θ will be developed in Fourier series and restricted on the first harmonics of the coordinate θ

$$F_1(R, \theta, z) = F_{10}(R, z) + F_{11}(R, z) \cos \theta + F_{12}(R, z) \sin \theta \quad (7)$$

In this sequence the three dimensional variables $F(R, \theta, z)$ are transformed to a group of two dimensional variables $F_0, F_{10}, F_{11}, F_{12}$ which are coupled together.

Making use of equations (5)-(7) in equation (4) and collecting only the coefficients of the zeroth and first order terms of and the coefficients of the first harmonics $\cos \theta$ and $\sin \theta$, we get three groups of equations. Expressing the variables which have the form F_{11}, F_{12} by the form F_1 and F_2 and to make the handling of these equations does not need very long discretising forms and many special forms in the numerical solution these three groups of equations will be expressed by using a number of operators for the special terms as follows:

$$\begin{aligned} \frac{\partial \vec{u}_0}{\partial t} &= N_0(\vec{u}_0, w_g) - G_0 P_0 \\ \frac{\partial \vec{u}_1}{\partial t} &= N_1(\vec{u}_1, \vec{u}_0, w_g) + M_1(\vec{u}_2, \vec{u}_0, P_0) - G_0 P_1 - G_1 P_2 \\ \frac{\partial \vec{u}_2}{\partial t} &= N_1(\vec{u}_2, \vec{u}_0, w_g) + M_2(\vec{u}_1, \vec{u}_0) - G_0 P_2 + G_1 P_1 \end{aligned} \quad (8)$$

and the continuity equations as follows:

$$\begin{aligned} D_0 \vec{u}_0 + \frac{1}{Q} \frac{dQ}{dt} &= 0 \\ D_0 \vec{u}_1 + D_1 \vec{u}_2 - 2R \frac{\partial u_0}{\partial R} &= 0 \\ D_0 \vec{u}_2 - D_1 \vec{u}_1 - 2v_0 &= 0 \end{aligned} \quad (9)$$

where $\vec{u}_0 = \begin{bmatrix} u_0 \\ v_0 \\ w_0 \end{bmatrix}$, $\vec{u}_1 = \begin{bmatrix} u_1 \\ v_1 \\ w_1 \end{bmatrix}$ and $\vec{u}_2 = \begin{bmatrix} u_2 \\ v_2 \\ w_2 \end{bmatrix}$

The definitions of the convection operators N_0, N_1, M_1, M_2 , the gradient operators G_0, G_1 and the divergent operators D_0, D_1 can be expressed by using \vec{a}, \vec{u}, g, f for the vector and scalar quantities as follows:

$$N_0(\vec{u}, g) = -u \frac{\partial \vec{u}}{\partial R} + (g-w) \frac{\partial \vec{u}}{\partial z} + \begin{bmatrix} v^2/R \\ -uv/R \\ 0 \end{bmatrix} \quad (10)$$

$$N_1(\vec{a}, \vec{u}, g) = -u \frac{\partial \vec{a}}{\partial R} + (g-w) \frac{\partial \vec{a}}{\partial z} - a \frac{\partial \vec{u}}{\partial R} - c \frac{\partial \vec{u}}{\partial z} + \begin{bmatrix} 2v.b/R \\ -(u.b+v.a)/R \\ 0 \end{bmatrix} \quad (11)$$

$$M_1(\vec{a}, \vec{u}, f) = 2R u \frac{\partial \vec{u}}{\partial R} - \begin{bmatrix} 1 \\ 0 \\ 0 \end{bmatrix} \cdot 2R \cdot \frac{\partial f}{\partial R} - \frac{1}{R} v \cdot \vec{a} \quad (12)$$

$$M_2(\vec{a}, \vec{u}) = \frac{1}{R} v \cdot \vec{a} + 2 \begin{bmatrix} u \cdot v \\ -u^2 \\ 0 \end{bmatrix} \quad (13)$$

$$D_0 \vec{a} = \frac{1}{R} \frac{\partial(a.R)}{\partial R} + \frac{\partial(c.R)}{\partial z} \quad \text{and} \quad D_1 \vec{a} = \frac{b}{R} \quad (14)$$

$$G_0 f = \begin{bmatrix} \frac{\partial f}{\partial R} \\ 0 \\ \frac{\partial f}{\partial z} \end{bmatrix} \quad \text{and} \quad G_1 f = \begin{bmatrix} 0 \\ f/R \\ 0 \end{bmatrix} \quad (15)$$

$$\text{where } \vec{a} = \begin{bmatrix} a \\ b \\ c \end{bmatrix} \quad \text{and} \quad \vec{u} = \begin{bmatrix} u \\ v \\ w \end{bmatrix}$$

2.5 The Boundary and initial conditions

The boundary conditions express the global features of the in-cylinder flow, only special condition occurs at the axis. The velocities u_1 and v_2 and also u_2 and v_1 are coupled together in such a way to make the velocity contours smoothly flow along the axis. These boundary conditions are summarized as follows:

- $u_0 = v_0 = 0, u_1 + v_2 = 0, u_2 + v_1 = 0, w_1 = w_2 = 0, \partial w_0 / \partial R = 0$ at the axis
- $u_0 = u_1 = u_2$ at the cylinder and bowl walls
- $w_0 = w_1 = w_2$ at the cylinder top
- $w_0 = w_p, w_1 = w_2 = 0$ at the piston crown and bowl bottom
- $\partial p_0 / \partial n = 0$ at all boundaries,
- $p_1 = p_2 = 0$ at the axis while $\partial p_1 / \partial n = \partial p_2 / \partial n = 0$ at all other boundaries. where n is the normal coordinate to the boundary.

The initial conditions are given to the quantities at the time of inlet valve closing as a forced vortex having a swirl ratio ω_0 which is assumed to be constant in the axial direction.

3. SOLUTION ALGORITHM

3.1 Method of solution

For the numerical time integration there are many methods, but to make the required computer capacity not very big the simplest explicit one direction forward method will be used and the value of the velocity vector \vec{u}_0 , \vec{u}_1 and \vec{u}_2 at the time $t+\delta t$ is calculated from the velocity vectors \vec{u}'_0 , \vec{u}'_1 and \vec{u}'_2 at the time t

$$\vec{u}_1 = \vec{u}'_1 + \delta t \frac{\partial \vec{u}'_1}{\partial t} \quad (16)$$

$\frac{\partial \vec{u}'_1}{\partial t}$ can be calculated only when the pressure is known. Because the pressure is not known at first, the following algorithm will be used.

From the fact that the new \vec{u}_1 at the time $t+\delta t$ must satisfy the continuity equations (9), then by substituting \vec{u}_1 in these equations it will take the following form

$$\begin{aligned} D_0 \vec{u}_0 + \frac{1}{\rho} \frac{d\rho}{dt} &= D_0 (\vec{u}'_0 + \delta t \frac{\partial \vec{u}'_0}{\partial t}) + \frac{1}{\rho} \frac{d\rho}{dt} = 0 \\ D_0 \vec{u}_1 + D_1 \vec{u}_2 - 2R \frac{\partial u_0}{\partial R} &= D_0 [\vec{u}'_1 + \delta t \frac{\partial \vec{u}'_1}{\partial t}] + D_1 [\vec{u}'_2 + \delta t \frac{\partial \vec{u}'_2}{\partial t}] - 2R \frac{\partial u'_0}{\partial R} = 0 \\ D_0 \vec{u}_2 - D_1 \vec{u}_1 - 2v_0 &= D_0 [\vec{u}'_2 + \delta t \frac{\partial \vec{u}'_2}{\partial t}] - D_1 [\vec{u}'_1 + \delta t \frac{\partial \vec{u}'_1}{\partial t}] - 2v'_0 = 0 \end{aligned} \quad (17)$$

Taking into consideration equation (16) and with the use of the relations

$$\begin{aligned} \vec{q}_0 &= \vec{u}'_0 + \delta t N_0(\vec{u}'_0, w_g) \\ \vec{q}_1 &= \vec{u}'_1 + \delta t [N_1(\vec{u}'_1, \vec{u}'_0, w_g) + M_1(\vec{u}'_2, \vec{u}'_0, P_0)] \\ \vec{q}_2 &= \vec{u}'_2 + \delta t [N_1(\vec{u}'_2, \vec{u}'_0, w_g) + M_2(\vec{u}'_1, \vec{u}'_0)] \end{aligned} \quad (18)$$

for the convection term and also

$$p_0 = \delta t.P_0, \quad p_1 = \delta t.P_1 \quad \text{and} \quad p_2 = \delta t.P_2 \quad (19)$$

equation (17) will give for the pressure the following relations

$$\begin{aligned} D_0 G_0 p_0 &= D_0 \vec{q}_0 + \frac{1}{\rho} \frac{d\rho}{dt} \\ (D_0 G_0 - D_1 G_1) p_1 &= D_0 \vec{q}_1 + D_1 \vec{q}_2 - 2R \frac{\partial \vec{u}'_0}{\partial R} \\ (D_0 G_0 - D_1 G_1) p_2 &= D_0 \vec{q}_2 - D_1 \vec{q}_1 - 2v'_0 \end{aligned} \quad (20)$$

Equation (20) is an elliptic equation from Poisson's type and is used to calculate p by the known right hand side. This equation will be solved by iteration by using the ADI method [8]. By the calculated value of p the velocity \bar{u}_i can be calculated by the equation (21).

$$\begin{aligned}\bar{u}_0 &= \bar{q}_0 - G_0 p_0 \\ \bar{u}_1 &= \bar{q}_1 - G_0 p_1 - G_1 p_2 \\ \bar{u}_2 &= \bar{q}_2 - G_0 p_2 + G_1 p_1\end{aligned}\quad (21)$$

3.2 Diskretisation of the differential equations

For the discretisation of the governing equations two different two dimensional staggered grids in the way discussed by Stephens et al [9] are used for the vector and scalar variables as shown in Fig. 5. The crosses (+) represent the points of the grid Ω_G for the vector field and the points (.) represent the point of the grid $\tilde{\Omega}_G$ for the scalar field. The calculation of the convection terms and the pressure gradient will be at the points of the grid Ω_G and the satisfaction of the continuity equation will be at the points of the grid $\tilde{\Omega}_G$. Variable axial spacing is used to allow for the change of the distance between the cylinder head and the piston crown, while a fixed grid system is used for the space in the piston bowl. The number of the axial nodes is varied during compression to avoid the extremely small spacing between it [1].

To express the discrete operation which are used in equations (17)-(21) without making many special forms, the following definitions will be taken into consideration

$$\begin{aligned}(a)^+ &= \begin{cases} a & \text{for } a > 0 \\ 0 & \text{for } a \leq 0 \end{cases}, \quad d_k = \begin{cases} d_c & \text{for } 1 \leq k < L_3 \\ d_b & \text{for } L_3 \leq k \leq L_4 \end{cases} \\ w_{gk} &= \begin{cases} w_p (k-1)/(L_3-1) & \text{for } k \leq L_3 \\ w_p & \text{for } k \geq L_3 \end{cases} \\ R_1 &= (1-1) d_R, \quad \tilde{R}_1 = (1 - \frac{1}{2}) d_R\end{aligned}$$

The convective operators N_0 , N_1 , M_1 and M_2 will take the following discrete forms

$$\begin{aligned}
 [N_0(\vec{u}, w_g)]_{i,k} &= \frac{1}{d_R} [(u_{i,k})^+ \cdot (\vec{u}_{i-1,k} - \vec{u}_{i,k}) + (-u_{i,k})^+ \cdot (\vec{u}_{i+1,k} - \vec{u}_{i,k})] \\
 &+ \frac{1}{d_{k-1}} (w_{i,k} - w_{gk})^+ \cdot (\vec{u}_{i,k-1} - \vec{u}_{i,k}) \\
 &+ \frac{1}{d_k} (w_{gk} - w_{i,k})^+ \cdot (\vec{u}_{i,k+1} - \vec{u}_{i,k}) + \frac{1}{R_1} \begin{bmatrix} v_{i,k}^2 \\ -u_{i,k} v_{i,k} \\ 0 \end{bmatrix} \quad (22)
 \end{aligned}$$

$$\begin{aligned}
 [N_1(\vec{a}, \vec{u}, w_g)]_{i,k} &= \frac{1}{d_R} [(u_{i,k})^+ \cdot (\vec{a}_{i-1,k} - \vec{a}_{i,k}) + (-u_{i,k})^+ \cdot (\vec{a}_{i+1,k} - \vec{a}_{i,k})] \\
 &+ \frac{1}{d_{k-1}} (w_{i,k} - w_{gk})^+ \cdot (\vec{a}_{i,k-1} - \vec{a}_{i,k}) + \frac{1}{d_k} (w_{gk} - w_{i,k})^+ \cdot (\vec{a}_{i,k+1} - \vec{a}_{i,k}) \\
 &+ \frac{a_{i,k}}{2 \cdot d_R} (\vec{u}_{i-1,k} - \vec{u}_{i+1,k}) \\
 &+ \frac{a_{i,k}}{d_{k-1} + d_k} (\vec{u}_{i,k-1} - \vec{u}_{i,k+1}) + \frac{1}{R_1} \begin{bmatrix} 2v_{i,k} \cdot b_{i,k} \\ -u_{i,k} \cdot b_{i,k} - v_{i,k} \cdot a_{i,k} \\ 0 \end{bmatrix} \quad (23)
 \end{aligned}$$

$$\begin{aligned}
 [M_1(a, u, f)]_{i,k} &= \frac{2R_1}{d_R} [(u_{i,k})^+ \cdot (\vec{u}_{i,k} - \vec{u}_{i-1,k}) + (-u_{i,k})^+ \cdot (\vec{u}_{i,k} - \vec{u}_{i+1,k})] \\
 &- \frac{v_{i,k} \cdot \vec{a}_{i,k}}{R_1} - \frac{2R_1}{d_{k+1} + d_k} \begin{bmatrix} 1 \\ 0 \\ 0 \end{bmatrix} [d_k (f_{i,k-1} - f_{i-1,k-1}) + d_{k-1} (f_{i,k} - f_{i-1,k})] \quad (24)
 \end{aligned}$$

$$[M_2(a, u)]_{i,k} = \frac{1}{R_1} \cdot v_{i,k} \cdot \vec{a}_{i,k} + 2 \begin{bmatrix} u_{i,k} \cdot v_{i,k} \\ -u_{i,k}^2 \\ 0 \end{bmatrix} \quad (25)$$

and the discrete forms for the gradient fields $G_0 f$ and $G_1 f$ will be

$$[G_0 f]_{i,k} = \frac{1}{d_R(d_{k-1} + d_k)} \begin{bmatrix} d_{k-1}(f_{i,k} - f_{i-1,k}) + d_k(f_{i,k-1} - f_{i-1,k-1}) \\ 0 \\ d_R(f_{i,k} + f_{i-1,k} - f_{i,k-1} - f_{i-1,k-1}) \end{bmatrix}$$

$$[G_1 f]_{i,k} = \begin{bmatrix} 0 \\ 1 \\ 0 \end{bmatrix} \frac{d_{k-1}(f_{i,k} + f_{i-1,k}) + d_k(f_{i,k-1} + f_{i-1,k-1})}{2 R_1 (d_{k-1} + d_k)} \quad (26)$$

(27)

Fig. 6 shows the values of the function f which is used in equations (26) and (27) to calculate the gradient fields $G_0 f$ and $G_1 f$ at the point $P_{i,k} \in \tilde{S}_G$

Fig. 7 shows the velocity components which are used to calculate the discrete forms of the diverging operators $D_0 \vec{u}$ and $D_1 \vec{a}$ at the point $P_{i,k} \in \tilde{S}_G$ according to the definition of equation (14) as follows

$$\begin{aligned} [D_0 \vec{u}]_{i,k} = & \frac{1}{2R_i} \left\{ \frac{R_{i+1}}{d_R} (u_{i+1,k} + u_{i+1,k+1}) - \frac{R_i}{d_R} (u_{i,k} + u_{i,k+1}) \right\} \\ & + \frac{R_{i+1}}{d_k} (w_{i+1,k+2} - w_{i+1,k}) + \frac{R_i}{d_k} (w_{i,k+1} - w_{i,k}) \end{aligned} \quad (28)$$

$$[D_1 \vec{a}]_{i,k} = \frac{1}{4R_i} (b_{i+1,k+1} + b_{i+1,k} + b_{i,k+1} + b_{i,k}) \quad (29)$$

A computer program system EBSTR is written in FORTRAN for the numerical simulation of the in-cylinder flow during compression. The complete details and discussion for this system can be found in ref. [10].

4. CONCLUSIONS

This paper shows and describes a numerical method to simulate and predict the turbulent unsteady swirling flow in an eccentric deep bowl combustion chamber of an engine cylinder during compression stroke. The three dimensional problem could be transformed to a number of two dimensional problems by the perturbation method to adopt the present computer capacity. The numerical simulation is performed by using the finite difference method. This method has been applied to simulate the two dimensional flow in a symmetrical deep bowl combustion chamber [1] and the three dimensional flow in an eccentric deep bowl combustion chamber of a direct injection diesel engine in the second part of this paper [11].

5. NOMENCLATURE

a	Eccentricity of the bowl axis
b_1	Bowl height (depth)
c_1	Total cylinder length = h at BDC
d_b, d_c	Grid spacing in z direction in the bowl and cylinder
d_R	Grid spacing in R direction
D_0, D_1	Divergent operators
f	Scalar field
F	Dependent variable
G_0, G_1	Gradient operators
h	Piston position from the cylinder top
$L_1 \dots L_4$	Number of grid points in R and z direction
M_1, M_2	Convection operators
N_0, N_1	Convection operators
P	Pressure per unit density

R	Radial coordinate in the R plane
t	time
u, v, w	Velocity components in the R, θ and z coordinates
U, V, W	Velocity components in the X, Y and z coordinates
w	Complex variable in the plane $z=\text{constant}$
w_g, w_p	Grid points and piston velocities
x, y	Cartesian coordinates
X, Y, z	Oriented cartesian coordinates
x', z'	Fixed and movable coordinates
β	Angle between the coordinates $R=\text{const}$ and $X=\text{const}$.
E	Eccentricity parameter
ζ	Complex variable in the plane $z=\text{const}$. ($\zeta = \xi + i\eta$)
θ	Tangential coordinate
ρ	Density
ω_0	Swirl ratio, the ratio of swirl angular velocity of that of the engine shaft

6. REFERENCES

1. El Kady, M.S., Mascheck, H.J., and HOCHÉ, A., "Numerical simulation of the flow in a symmetrical deep bowl combustion chamber of a diesel engine cylinder during the compression stroke. MEJ, Vol. 12, No. 2, Dec. 1987, pp M20-M30
2. Gosman, A.D. and John, R.J.R., SAE paper No. 800091 (1980).
3. Ramos, J.I., Humphera, J.A.C. and Sirignano, N.A., SAE paper No. 790356 (1979).
4. Griffin, M.D., Anderson, J.D., Diwaker, R., "Navier-Stokes solution of flow field in an I.C.E." AIAA Journal, Vol 14 Dec. 1976 pp 1665-1666.
5. Diwakar, R., Anderson, J.D., Griffin, M.D., "Inviscid solutions of the flow field in an I.C.E." AIAA Journal, Vol 14 Dec. 1979 pp 1667-1668
6. Seppen, J.J., "A study of flow field phenomena in I.C.E." Ph.D. thesis, TH Delft, October 1982.
7. El Kady, M.S., "Berechnung symmetrischer und unsymmetrischer Zylinder-Brennraum-Stroemungen in Dieselmotoren beim Verdichtungshub" Dissertation, TU Dresden March 1985
8. Peaceman, D.W., Rachford, H.H., "The numerical solution of parabolic and elliptic differential equations", J.Soc. Indust. Appl. Math. 3, 28-41, 1955.
9. Stephens, A.S., Bell, J.B., Solomon, J.M., "A finite difference formulation for the incompressible Navier-Stokes equation" J. of computational physics, vol. 5 (1984) pp 152-172.
10. El Kady, M.S., "Anleitung zur Nutzung der Programme fuer die Berechnung der Zylinder-Brennraum-Stroemungen in Dieselmotoren beim Verdichtungshub." Bericht No. 656. TU Dresden Sektion 12, WB Stroemungstechnik.
11. El Kady, M.S., Mascheck, H.J. and Hoche, A., "Numerical simulation of flows in an engine cylinder with an eccentric deep bowl combustion chamber during compression " (2nd Report: numerical example) MEJ, Vol. 16, No. 2 Dec 1989

Fig. 1
The integration area

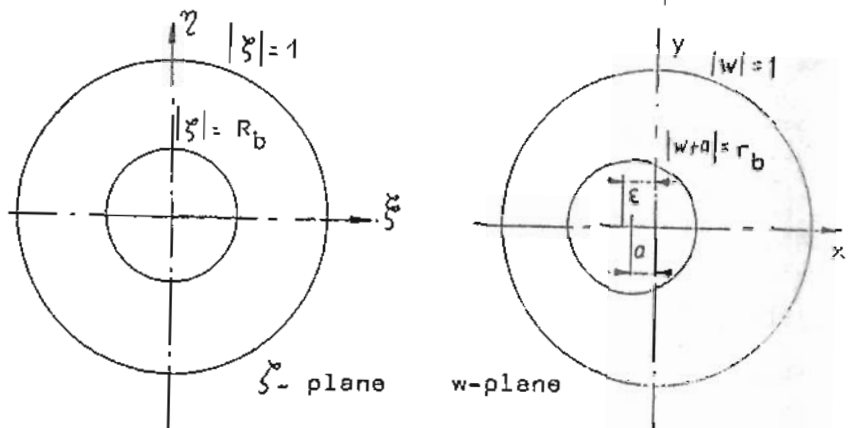
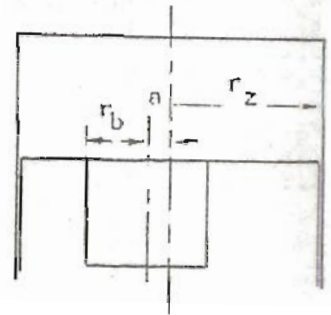


Fig. 2 conformal mapping for the z-plane

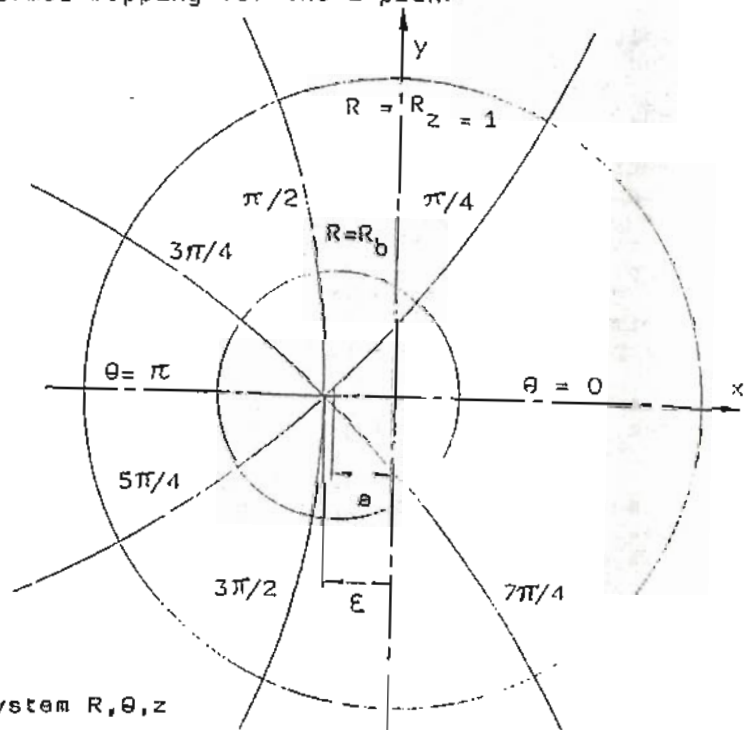


Fig. 3
The coordinate system R, θ, z

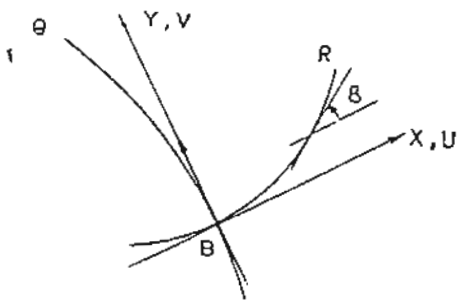


Fig. 4
The oriented cartesian coordinate X, Y, Z

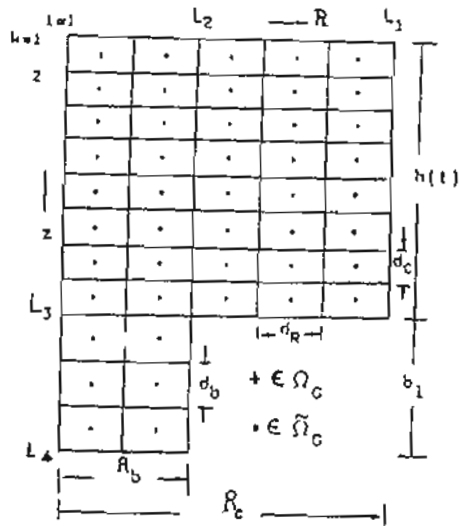


Fig. 5
The computational arrangement

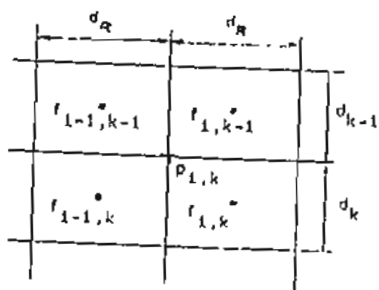


Fig. 6
The values of the function f which is used to calculate the gradient fields $G_0 f$ and $G_1 f$

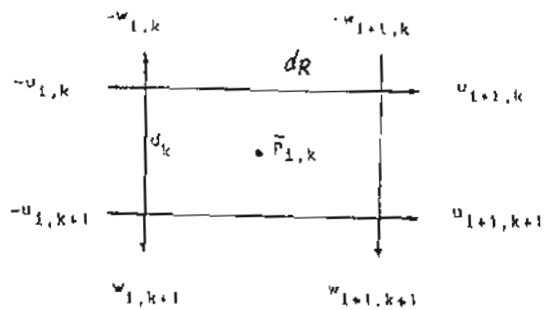


Fig. 7
The velocity components which is used to calculate the discrete values $D_0 u$ and $D_1 u$